Geometric accuracy evaluation and analysis of ZY-1 02E IRS thermal infrared image data using GCP extraction based on phase correlation matching method

Liping Zhao [1], Xianhui Dou [1], Fan Mo [1], Hongmo Li [2], Fangxu Zhang [1], Dian Qu[1],Junfeng Xie [1,*]

[1] Land Satellite Remote Sensing Application Center, Ministry of Nature Resource, Beijing, China - zhaolpwww@163.com, douxianhui@lasac.cn, mofan@lasac.cn, fangxv_zhang@163.com, qdjzqd0401@163.com, xiejf@lasac.com
[2] School of Surveying and Geographical Science, Liaoning Technical University, Fuxin, Liaoning, China - 2465905651@qq.com

Keywords: ZY-1 02E IRS, Thermal Infrared Image, Phase Correlation Matching, GCP extraction, Geometric Accuracy.

Abstract

The Ziyuan-1 (ZY-1) 02E launched on December 26, 2021 is equipped with a thermal infrared sensor (IRS), which has a ground resolution of better than 16m and a width priority of 115km, balancing the advantages of high resolution and large wide observation. The geometric performance of image data is the premise of remote sensing application, and the difficulty in evaluating the geometric performance of thermal infrared image data lies in the extraction of well-distributed, reliable and accurate GCPs. To extract GCP from high-precision reference images, it is necessary to overcome the feature differences between images caused by different spectral responses. This paper adopts a phase correlation matching method based on frequency domain to realize the fine registration of the data obtained by the emission thermal spectral band with the data from the reflectance spectral band, which can not only solve the GCP extraction of conventional thermal infrared images collected during the day, but also obtain satisfactory GCP data from thermal infrared data acquired at night. In order to test the GCP method proposed in this paper, three typical areas are selected as the experimental areas, including Yiyang City in Hunan, Nagqu City in Xizang and Hami City in Xinjiang, and the internal geometric accuracy and absolute geolocation accuracy of the thermal infrared data spanning one year are evaluated and analyzed by using the reference data composed of the DOM with an accuracy of 2m and the DEM with an accuracy of 10m. The research results indicate that the internal geometric accuracy of ZY-1 02E IRS satellite image data is better than 1.0 pixels, and the performance is satisfactory. However, its absolute geolocation accuracy needs to be continuously improved, especially there are systematic errors in the ascending data at night that require further research. Overall, it meets the design accuracy indicators of satellites and can meet the application requirements of thermal infrared remote sensing.

1. Introduction

The Ziyuan-1 (ZY-1) 02E launched on December 26, 2021 is equipped with three main payloads, including a 9-band visible near-infrared camera (VNIC), a 166-band hyper-spectral imager, and a single-band thermal infrared sensor (IRS). It is also known as the 5m Optical 02 Satellite, which is the successor satellite of ZY-1 02D, and they are all important components of China's space-based infrastructure to continue to carry out the moderate resolution Earth observation missions. It is mainly devoted to providing panchromatic, multispectral, hyper-spectral and thermal infrared data for the operation of natural resource monitoring and management, disaster prevention and control, environmental protection, etc. The ZY-1 02E has added the IRS compared to its predecessor, which has a ground resolution of better than 16m and a width priority of 115km, taking into account the advantages of high resolution and large wide observation. The IRS mainly collect thermal radiation information about the target and can work all day.

In order to ensure the high quality of radiometric and geometrically corrected image data, geometric accuracy and radiometric quality need to be evaluated and verified. Among them, absolute geolocation accuracy, internal geometric accuracy and band registration accuracy are the most important geometric performance indicators, which are the main contents of geometric calibration and verification activities, and these performance indicators need to be continuously verified, monitored and improved.

Geometric accuracy analysis is a challenge for thermal infrared image data, and the main problem is that it is difficult to obtain satisfactory tie-points between the reference data of the reflective bands and the long-wave thermal infrared emissive bands.

For the Landsat 8 and Landsat 9 the Thermal Infrared Sensor (TIRS) geometric characterization and calibration, the Operational Land Imager (OLI) short-wave infrared (SWIR) band image acquired simultaneously with TIRS is used as a reference, and the normalized gray scale correlation with a surface fitting polynomial algorithm is utilized to extract the tie-points (Storey J. et al., 2014; Choate, M.J. et al., 2023; Choate, M.J. et al., 2024). In other words, the geometric performance analysis of Landsat 8 and Landsat 9 TIRS is premised on the rigid constraints between SWIR and TIRS, so a well-calibrated OLI is a prerequisite for on-orbit geometric analysis of TIRS.

For the ZY-1 02E IRS thermal infrared image data, this paper adopts the phase-correlated matching method based on frequency domain to achieve the accurate registration between the data obtained by the emission spectral band and the data of the reflectance spectral band, and further analyzes the geometric performance of the thermal infrared image, especially for the nighttime imaging data, and carries out a reliable geometric accuracy evaluation and analysis for the first time.

2. Geometric Model

2.1 Spacecraft and IRS Overview

The ZY-1 02E satellite orbits the Earth in a sun-synchronous, at an altitude of 778 km, inclined at 98.5 degrees. The satellite has a 55-day repeat cycle with an equatorial crossing time: 10:30 a.m. Table 1 summarize the main characteristics of the ZY-1 02E.

The IRS adopts long-line array push-broom imaging, which has better sensitivity than traditional scanning imaging and can obtain ground object temperature information more accurately. Moreover, it is a push-broom sensor with no moving parts, and there is no influence of mechanism swing in the imaging process, which helps to improve the geometric performance of the image. The IRS optical system adopts a catadioptric optical system, including the main optical system and the relay optical system, the optical system has a pupil diameter of 435mm, a focal length of 1038mm, and a field of view of 8.6° in the push-sweeping direction. With high-precision thermal control technology, the stability design index of the internal azimuth element is ensured, and the absolute distortion is less than 1μm. In addition, the infrared payload arranges a double-line detector in the focal plane, which can obtain two staggered images at the same time, and has the ability of super-resolution imaging. As shown in Figure 1, the thermal infrared camera detector is composed of 8 single-module detectors spliced together according to the zigzag structure, and the total number of pixels in the linear array direction reaches 8192 pixels, and the pixel size is 20 μm × 20 μm (Tong et al., 2023). The main specifications for the design of the IRS instrument are given in Table 2.

Item	Metrics
Launch date	December 26, 2021
Orbit type	Sun synchronous return orbit
Altitude	778 km
Inclination	98.5°
Descending intersection local time	10:30AM
Cycle	55 days
Pointing capability in cross-track	±32°
Design life	8 years

Table 1. Main characteristics of the ZY-1 02E

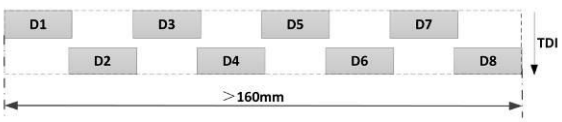

Figure 1. Long array focal plane stitching model (Tong et al., 2023)

2.2 Geometric Model

The ZY-1 02E satellite calculates orbital coordinates through the GPS receiver system, and relies on the combination of high-precision gyroscope and star sensor to solve the attitude. After completing the internal geometry calibration and external geometry calibration of the IRS, the physical imaging model of the camera can be built using the orbital position, attitude data, and time system.

In order to facilitate the application of image data, the rational polynomial coefficients (RPC) models are often used instead of strict physical models. In this paper, the affine transformation model in image space based on the RPC is used to study the geometric accuracy of the IRS.

Item	Specification
Spectral range	770-1050 nm
Focal length	1038mm
FOV (Filed of View)	≥8.6°
Pixel size	20 μm × 20 μm
GSD at nadir	≤16 m
Swath width	≥115 km
NETD	≤ 0.1K@300K
Dynamic range	240 K~340K
Static MTF	≥ 0.15@nyquist frequency
Absolute radiometric calibration accuracy	≤ 1K@300K
Relative radiometric calibration accuracy	≤ 3%
Quantization bits	12 bits
Internal geometric calibration accuracy	≤ 1 pixel (1σ)
Internal geometric accuracy of images (with GCP)	≤ 1.5 pixel (1σ)
Absolute Geolocation accuracy (without GCPs)	100 m (CE90)

Table 2. Main technical specifications of IRS thermal infrared image

3. Datasets

In order to study the absolute geolocation accuracy and internal geometric accuracy of the IRS thermal infrared data, three typical areas are selected as experimental areas, including Hunan, Xizang and Xinjiang. The reference data for the area is composed of a 2m accurate DOM and a 10m accurate DEM, and the IRS imagery data spans the four seasons of the year.

3.1 Study Area

Referring to the historical weather conditions and regional data acquisition in China, and considering the characteristics of terrain undulation and land cover type, several experimental areas such as Yiyang City in Hunan Province, Nagqu City in Xizang and Hami City in Xinjiang are preferentially selected. The vegetation in the Hunan experimental area is abundant, and the surface characteristics are clear. The Xizang experimental area has a high altitude and simple land cover. The air in the Xinjiang experimental area is dry, and the land surface cover is mainly Gobi and the vegetation is scarce.

3.2 Reference Data

As shown in Table 3, the reference datasets for Hunan, Xizang, and Xinjiang are part of the datasets covering the entire range of China, with planimatric and elevation accuracy of 2.0m and 10m, respectively. The accuracy of the dataset is reliable, and it can meet the accuracy research of IRS data with 16m GSD.

3.3 IRS Thermal Infrared Image

In the experimental regions, a total of 80 scenes of thermal infrared data with good quality are used for accuracy analysis from 2022 to 2024, including 40 scenes of images obtained on descending passes mode during the day and 40 scenes of data

obtained on ascending passes mode at night. Figure 2 shows an example of a typical IRS images on descending and ascending passes mode in Yiyang City, Hunan Province.

Items	Sub items	Hunan	Xizang	Xinjiang
Number of Images	Descending (day)	16	16	8
	Ascending (night)	18	6	16
Longitude	Min	111.5°	89.9°	93.2°
	Max	113.6°	92.0°	95.7°
Latitude	Min	28.1°	30.7°	41.3°
	Max	30.0°	31.8°	42.4°
Height	Min	19 m	4476 m	325 m
	Max	502 m	5731 m	2463 m
Reference data	DOM GSD	2.0m	2.0m	2.0m
	DOM accuracy	2.0m	2.0m	2.0m
	DEM Grid	30m	30m	30m
	DEM accuracy	10m	10m	10m

Table 3. Basic information of the experimental area.

(a) The image obtained on descending passes mode during the day.

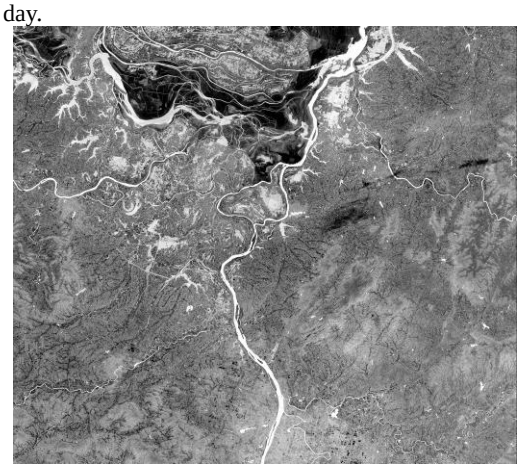

(b) The image obtained on ascending passes mode at night.

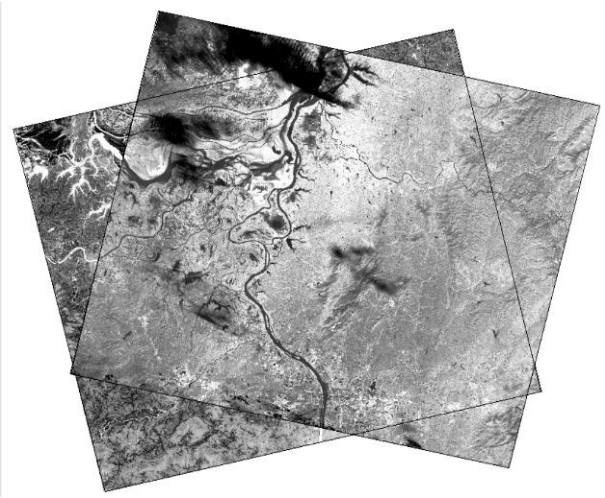

(c) The IRS images on descending and ascending passes mode overlaid by geographic coordinates

Figure 2. An example of a typical IRS images on descending and ascending passes mode in Yiyang City, Hunan Province.

4. GCP Extraction

Extracting GCP between emission thermal infrared image data and reflection spectral data using the matching method based on the spatial domain is difficult to obtain satisfactory tiepoints in most cases, while the phase correlation methods based on the frequency domain can generally achieve better results and can be used for studying the geometric accuracy of IRS data.

4.1 Phase correlation matching method

The principle of the phase correlation method (Kuglin and Hines, 1975) is based on the Fourier shift property, that is, when there is only a shift between the two image blocks, a linear phase difference will be reflected in the Fourier domain. The phase correlation image matching method uses the Fourier transform to convert the image blocks to be matched into the frequency domain for cross-correlation, which only uses the phase information in the mutual power spectrum of the frequency domain of the image blocks, which reduces the influence of the image grayscale value, has good anti-interference. It pays more attention to the texture information of the image, which can not only overcome the difficulty of matching caused by the change of ground coverage of multi-temporal images, but also eliminate the adverse effects brought by different image resolutions. It has excellent performance in the sub-pixel translation estimation of images with different properties and different spectral bands (Foroosh et al., 2002), and has better adaptability to thermal infrared image registration.

4.2 GCP Extraction Results

Figure 3, 4 and 5 show the Schematic diagram of GCP distribution of Hunan, Xizang and Xinjiang, respectively. Due to the rich texture of Hunan data, the GCP distribution is uniform and the extraction effect is very good, but for the data of Xizang and Xinjiang, the results of GCP extraction are acceptable and can be used for geometric accuracy evaluation, which will not affect the evaluation results, but it is still necessary to continue to explore and continuously improve the GCP extraction strategy in follow-up research.

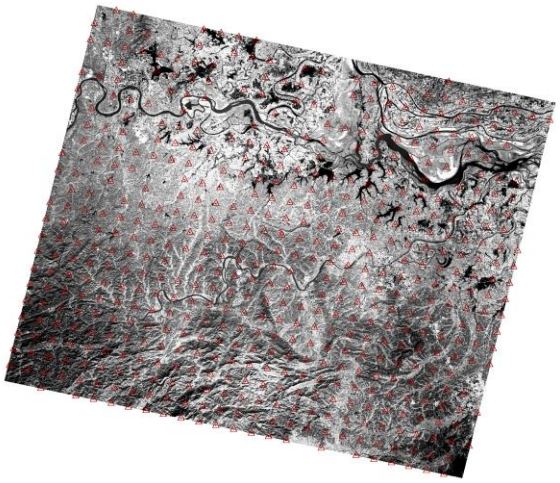

(a) Schematic diagram of GCP distribution of Hunan image data obtained on descending passes mode during the day.

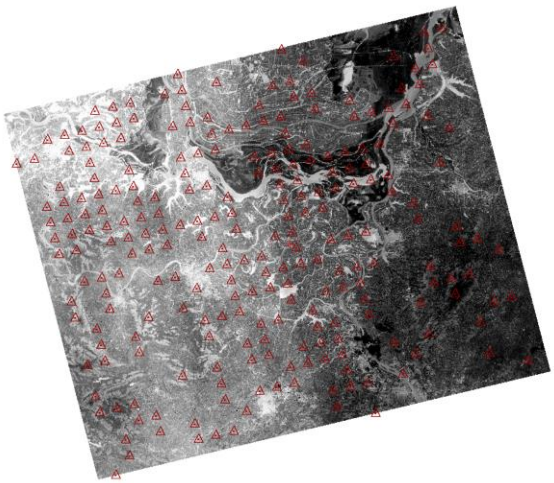

(b) Schematic diagram of GCP distribution of Hunan image data obtained on ascending passes mode at night.

Figure 3. Schematic diagram of GCP distribution of Hunan image data

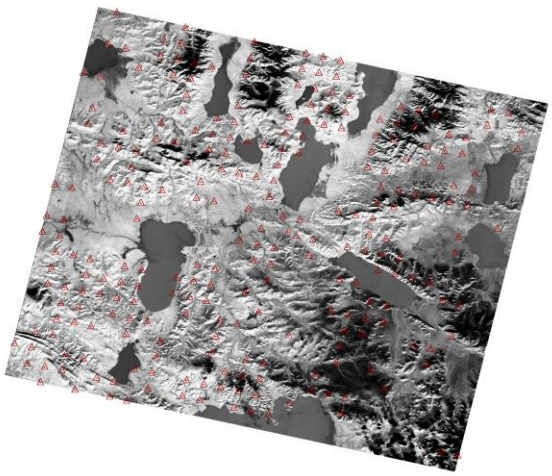

(a) Schematic diagram of GCP distribution of Hunan image data obtained on descending passes mode during the day.

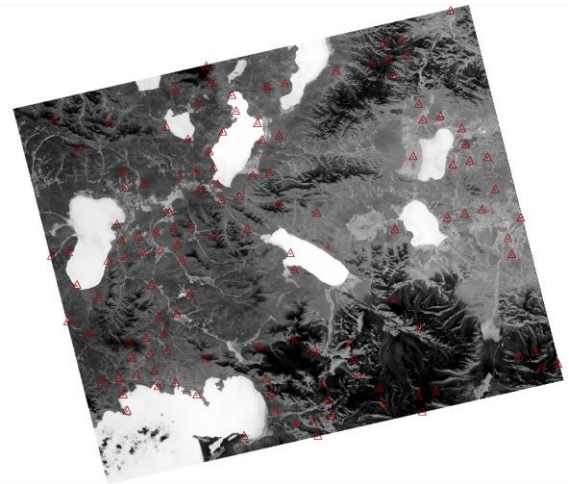

(b) Schematic diagram of GCP distribution of Hunan image data obtained on ascending passes mode at night.

Figure 4. Schematic diagram of GCP distribution of Xizang image data

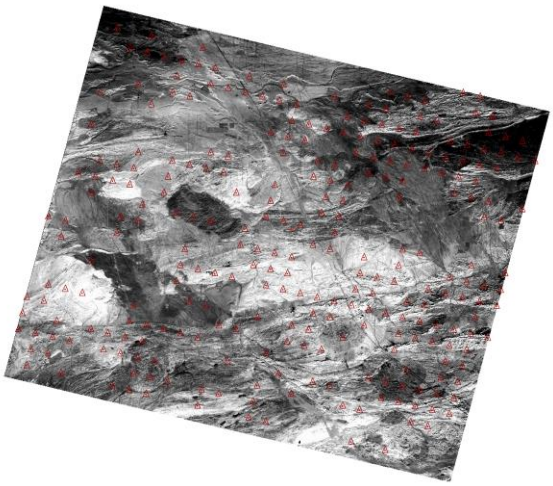

(a) Schematic diagram of GCP distribution of Hunan image data obtained on descending passes mode during the day.

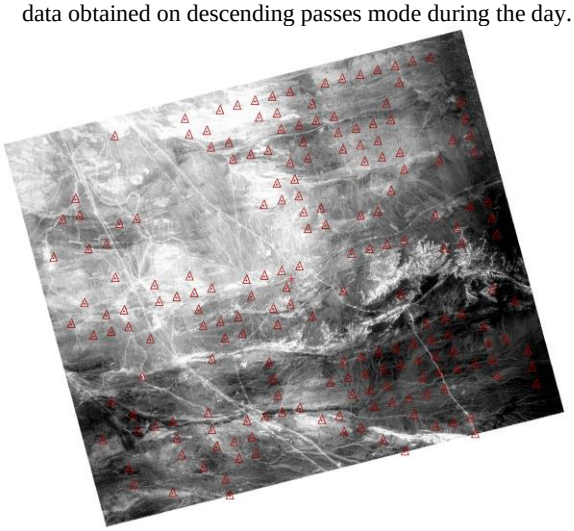

(b) Schematic diagram of GCP distribution of Hunan image data obtained on ascending passes mode at night.

Figure 5. Schematic diagram of GCP distribution of Xinjiang image data

5. Accuracy Evaluation

The internal geometric accuracy and absolute geolocation accuracy are evaluated using the IRS data of three test areas, including Hunan, Xizang, and Xinjiang.

5.1 Internal Geometric Accuracy

When all GCPs participate in the adjustment calculation, the internal geometric accuracy of the IRS image can be given by counting their residuals. Table 4 shows the internal geometric accuracy of the data of Hunan, Xizang and Xinjiang, respectively, and Figure 6 plots the RMS error distribution of each scene. In general, the accuracy is better than that of 1.0 pixels, and the accuracy of Hunan data is higher, which is presumably due to the better quality of GCP extraction. There is no significant difference in the accuracy of the data on descending and ascending passes mode.

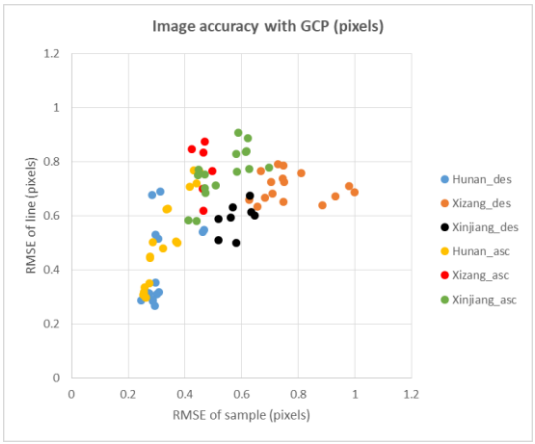

Figure 6. The internal geometric error distribution of each scene of Hunan, Xizang and Xinjiang (RMSE, in pixels).

Items	Sub items	Min			Max			Average		
		Sample	Line	Count	Sample	Line	Count	Sample	Line	Count
Hunan	Descending (day)	0.247	0.266	360	0.468	0.699	554	**0.310**	**0.408**	454
	Ascending (night)	0.253	0.296	205	0.450	0.768	514	**0.327**	**0.500**	350
Xizang	Descending (day)	0.627	0.634	119	0.998	0.792	260	**0.774**	**0.706**	183
	Ascending (night)	0.425	0.619	98	0.497	0.874	127	**0.465**	**0.773**	113
Xinjiang	Descending (day)	0.518	0.500	194	0.647	0.674	332	**0.583**	**0.589**	274
	Ascending (night)	0.413	0.582	139	0.698	0.909	284	**0.538**	**0.760**	208

Table 4. The internal geometric accuracy of the IRS image of Hunan, Xizang and Xinjiang (RMSE, in pixels).

Items	Sub items	Min			Max			Average		
		Easting	Northing	Count	Easting	Northing	Count	Easting	Northing	Count
Hunan	Descending (day)	-26.386	-39.218	360	6.931	122.827	554	**-14.435**	**17.178**	454
	Ascending (night)	5.645	38.369	205	51.193	83.343	514	**27.866**	**55.643**	350
Xizang	Descending (day)	-32.832	-40.597	119	9.928	70.422	260	**-17.298**	**-10.392**	183
	Ascending (night)	26.558	37.530	98	53.345	63.314	127	**38.451**	**50.301**	113
Xinjiang	Descending (day)	-32.459	-63.421	194	8.480	66.655	332	**-11.102**	**-9.236**	274
	Ascending (night)	-2.366	60.985	139	54.573	75.896	284	**33.746**	**70.704**	208

Table 5. The absolute geolocation accuracy of the IRS image of Hunan, Xizang and Xinjiang (mean error, in meters).

5.2 Absolute Geolocation Accuracy

The absolute geolocation accuracy of the IRS image can be calculated by using all GCPs as checkpoints. The absolute geolocation accuracy of the data from Hunan, Xizang, and Xinjiang is given in Table 4, and the error distribution of each image is plotted in Figure 7. In general, the geolocation accuracy is not high, and the accuracy of the data on descending passes mode in the three test areas is basically the same.

Figures 8 and 9 respectively show the absolute geolocation error distribution of each scene on descending and ascending passes mode It can be observed from the figure that there are significant systematic errors in the absolute geolocation accuracy of the data on ascending passes mode in both the easting and northing directions, especially in the northing direction, which needs to be further analyzed in subsequent research.

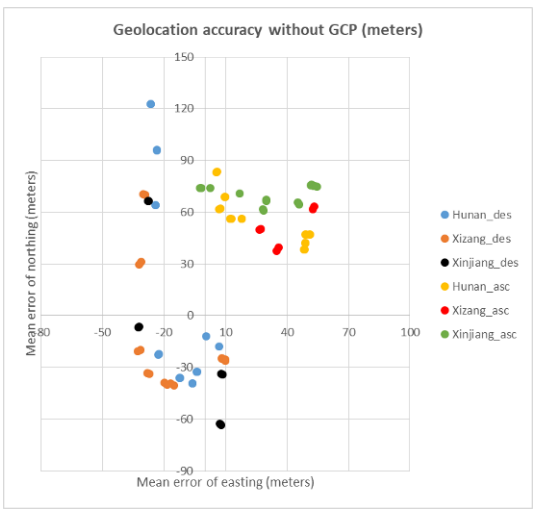

Figure 7. The absolute geolocation error distribution of each scene of Hunan, Xizang and Xinjiang (mean error, in meters).

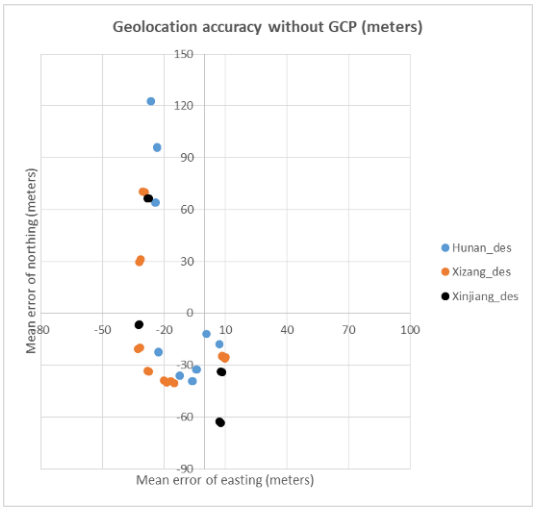

Figure 8. The absolute geolocation error distribution of each scene on descending passes mode of Hunan, Xizang and Xinjiang (mean error, in meters).

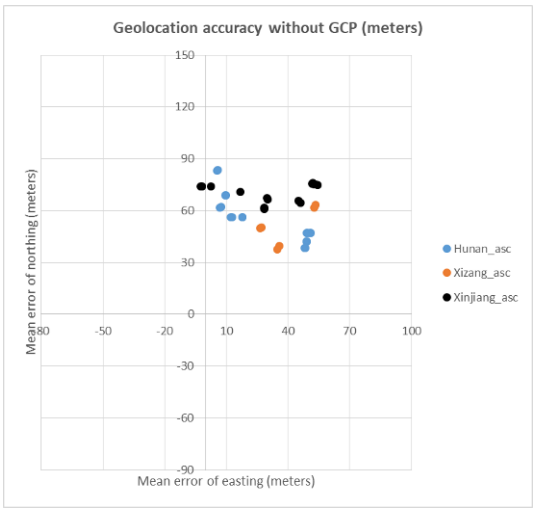

Figure 9. The absolute geolocation error distribution of each scene on ascending passes mode of Hunan, Xizang and Xinjiang (mean error, in meters).

6. Accuracy Analysis

After completing the IRS accuracy evaluation using the data from three experimental areas, further trend analysis is conducted on the internal geometric accuracy and absolute geolocation accuracy.

6.1 Internal Geometric Analysis

Figures 10 and 11 show the internal geometric error distribution of IRS data in the sample and line directions, respectively, based on the satellite roll angle and data acquisition date. Analysis of these graphs shows that there are no systematic errors related to the roll angle and the date of acquisition in both the descending and ascending orbit data.

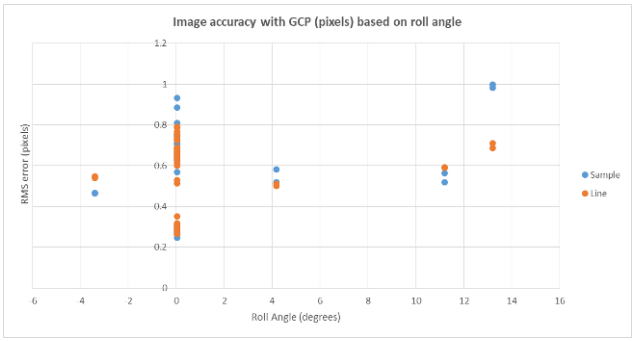

(a) The error distribution of the data obtained on descending passes mode during the day.

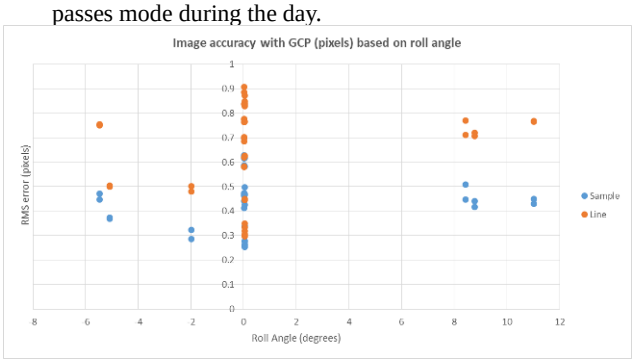

(b) The error distribution of the data obtained on ascending passes mode at night.

Figure 10. The internal geometric error distribution based on the roll angle (RMSE, in pixels).

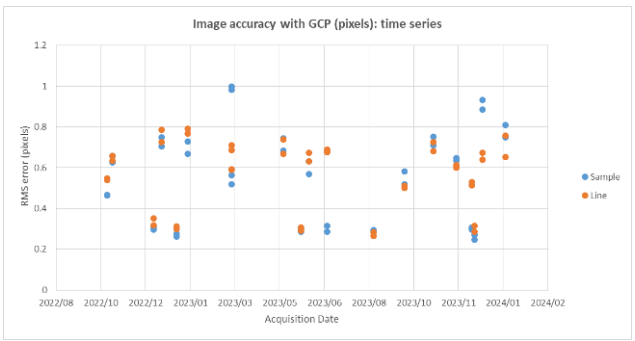

(a) The error distribution of the data obtained on descending passes mode during the day.

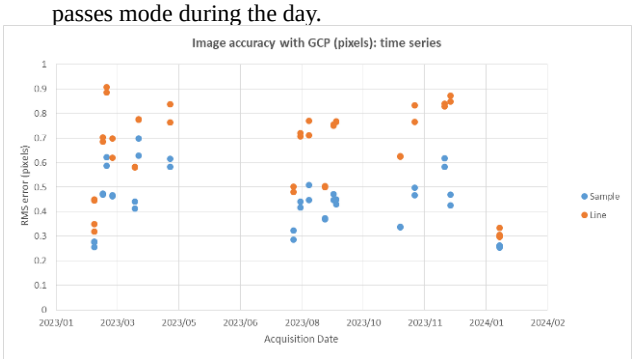

(b) The error distribution of the data obtained on ascending passes mode at night.

Figure 11. The internal geometric error distribution based on the acquisition date (RMSE, in pixels).

6.2 Absolute Geolocation Analysis

According to the satellite roll angle and the date of data acquisition, Figures 12 and 13 depict the absolute geolocation error distribution of IRS data in the easting and northing

directions, respectively. By observing these distribution, no systematic errors related to the roll angle and the date are found in the data on descending and ascending passes modes.

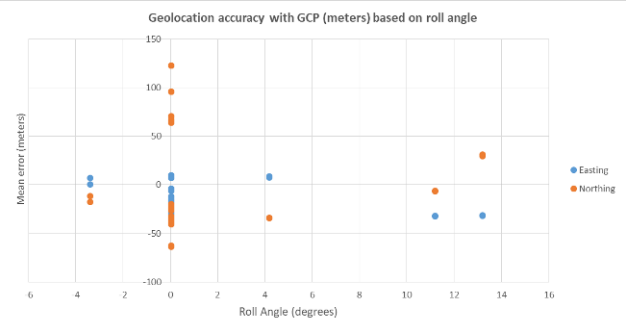

(a) The error distribution of the data obtained on descending passes mode during the day.

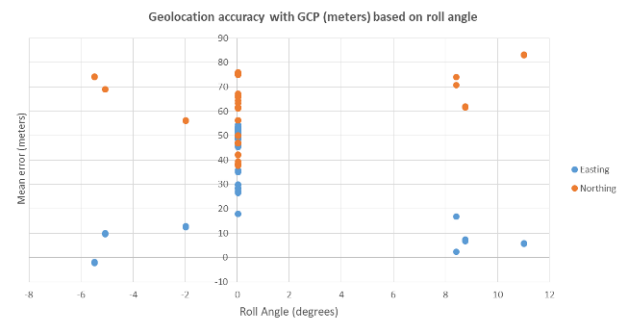

(b) The error distribution of the data obtained on ascending passes mode at night.

Figure 12. The absolute geolocation error distribution based on the roll angle (mean error, in meters).

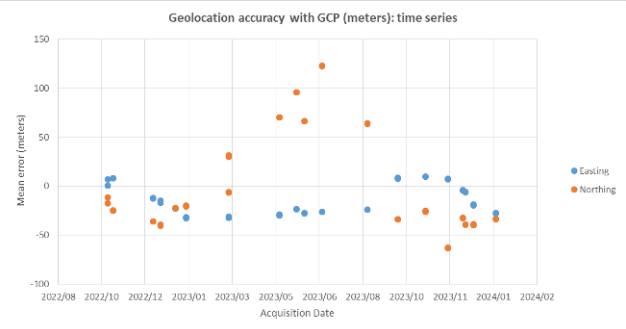

(a) The error distribution of the data obtained on descending passes mode during the day.

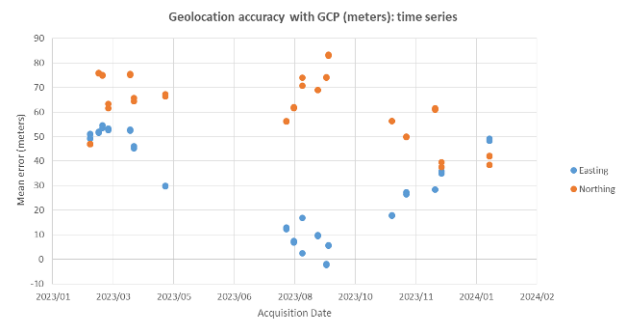

(b) The error distribution of the data obtained on ascending passes mode at night.

Figure 13. The absolute geolocation error distribution based on the acquisition date (mean error, in meters).

7. Conclusion

Aiming at the problem of analyzing the geometric performance of thermal infrared data of ZY-1 02E TIRS instrument, this paper uses the phase correlation matching algorithm based on frequency domain to solve the problem of reliable matching between the data obtained from the emission spectral band and the data of the reflectance spectral band, extracts satisfactory GCP data, and then carries out the evaluation and analysis of the geometric accuracy of thermal infrared image data using a total of 80 scenes data obtained in one year in experimental areas such as Hunan, Xizang and Xinjiang. For the first time, a relatively more accurate and reliable exploration of geometric characteristics has been carried out, especially for nighttime imaging thermal infrared remote sensing image data obtained on ascending passes mode.

The research results indicate that the internal geometric accuracy of IRS image data is good, which meets the specification indicators and can meet application requirements. In terms of absolute geolocation accuracy without GCP support, further improvement is needed, especially there are systematic errors in the ascending data at night, which requires research in the future. Although the absolute geolocation errors are more prominent compared with the widely used Landsat and Sentinel-2 data, the accuracy can be improved through the GCP, and the adverse effects on the remote sensing application of IRS thermal infrared data can be overcome.

References

Choate, M.J.; Rengarajan, R.; Storey, J.C.; Lubke, M. Landsat 9 Geometric Commissioning Calibration Updates and System Performance Assessment. *Remote Sens.* 2023, 15, 3524. https://doi.org/10.3390/rs15143524

Choate, M.J.; Rengarajan, R.; Hasan, M.N.; Denevan, A.; Ruslander, K. Operational Aspects of Landsat 8 and 9 Geometry. *Remote Sens.* 2024, 16, 133. https://doi.org/10.3390/rs16010133

Foroosh, Hassan, Zerubia, J. B., 2002. Extension of Phase Correlation to Sub-pixel Registration, *IEEE Transactions on Image Processing*, 11(3), 188-200.

James Storey, Michael Choate and Donald Moe. Landsat 8 Thermal Infrared Sensor Geometric Characterization and Calibration. *Remote Sens.* 2014, 6, 11153-11181. https://doi.org/10.3390/rs61111153

Kuglin, C. D and Hines D. C., 1975. The Phase Correlation Image Alignment Method, *in Proc. Int. Conf. Cybernetics Society*, 163-165.

TONG Weiming，LI Haoqian，NIE Yunsong，MA Jun，YAN Xiurong，XING Hui，GAO Changchun，WANG Baohua，SUN Qiyang，CAI Shuai，HAO Zhongyang，LI Yan. XXXX. Development of the high-resolution, high-sensitivity, large-width thermal infrared camera for 5m Optical 02 Satellite. *National Remote Sensing Bulletin*， XX(XX)：1-10 DOI： 10.11834/jrs.20232537. https://www.ygxb.ac.cn/thesis/91/35712176/zh/